Eur Biophys J (1993) 22: 71–77

European Biophysics Journal

Voltage clamp calculations for myelinated and demyelinated axons

Henry C. Tuckwell

School of Mathematical Sciences, Institute of Advanced Studies, Australian National University, GPO Box 4, Canberra ACT 2601, Australia

Received: 30 June 1992 / Accepted in revised form: 16 December 1992

Abstract. Exact cable theory is used to calculate voltage distributions along fully myelinated axons and those with various patterns of demyelination. The model employed uses an R-C circuit for the soma, an equivalent cable for the dendrites, a myelinated axon with n internodes and a cable representing telodendria. For the case of a voltage clamp at the soma, a system of $2n + 1$ equations must be solved to obtain the potential distribution and this is done for arbitrary n. An explicit calculation is performed for one internode whereas computer-generated solutions are obtained for several internodes. The relative importance of the position of a single demyelinated internode is determined. An approximate expression is given for the critical internodal length necessary for action potential generation.

Key words: Myelinated axons – Demyelination – Cable theory – Voltage calculations – Multiple sclerosis

Introduction

There have been many experimental and theoretical investigations of the electrophysiological properties and responses of myelinated nerve. In an early study, Rushton (1951) arrived at a relation between internodal length and the outer and inner diameter of the nerve fiber. A detailed analysis by Koide (1975) resulted in a formula for the characteristic length of myelinated nerve in terms of membrane and axoplasmic resistivities, diameters and internodal length. In an earlier analysis of cable model, Scott (1964) studied the relation of internodal length to velocity of propagation and found a linear relationship prevailed when the internodal length was large. Bement and Ranck (1969 a, b) performed an experimental and theoretical study of myelinated nerve in the dorsal column of cat. Using steady state cable theory for an infinite myelinated axon, they obtained reasonable fits to experimental data on such quantities as threshold current versus distance from an extracellular stimulating electrode.

Action potentials at nodal membrane were carefully subjected to analysis by Dodge and Frankenhaeuser (1958, and many subsequent papers) and a set of differential equations obtained for the transmembrane potential and ionic conductance variables by Frankenhaeuser and Huxley (1964). These equations are similar to the space-clamped Hodgkin-Huxley (1952) equations. In conjunction with passive models of internodes, such equations have been used to study action potential propagation in myelinated fibres (Moore et al. 1978; Waxman and Brill 1978). A somewhat surprising finding was that nodal properties had little effect on speed of conduction and that the latter was also insensitive to changes in internodal length.

An experimental model of demyelinated nerve which employed diphtheria toxin was studied by Rasminsky and Sears (1972). Internodal lengths in rat ventral root fibers ranged from 0.75 to 1.45 mm. It was found that, after demyelination, inward current still occurred only at nodes and that internodal conduction time increased by up to an order of magnitude. Cable properties of demyelinated internodes were altered as capacitance increased and transverse membrane resistance decreased. Furthermore, the refractory period increased. A companion theoretical study (Koles and Rasminsky 1972) employed the Frankenhaeuser-Huxley equations to calculate nodal voltages and a compartmental model for the internodes in a fibre with 21 nodes. Thus only ordinary rather than partial differential equations were used. The effects of altering the thickness of myelin were considered. As the thickness of the myelin was reduced in a single internode, the internodal conduction time increased until at 2.7% of normal thickness, conduction failed. A non-linear effect was noticed in that the demyelination of two internodes separated by a normal internode had more than double the effect of demyelinating just one internode. Propagation in a demyelinated fibre was calculated to be much more readily blocked by increased internal sodium or by increased temperature than in a normal fibre.

There have been several other studies of the theoretical aspects of myelinated nerve, including threshold effects (Bell 1980), effects of extracellular stimulation (Rubinstein 1991) and the stability of solutions of the associated differential equations (Chen 1992). Many experimental and

theoretical results of significance were discussed by Ritchie (1984a, b), including ion-channel properties and distributions. The study of models of myelinated axons is expected to be useful in helping to understand the effects of pattern of demyelination occuring in diseases such as multiple sclerosis (MS). In MS myelin sheaths are destroyed or degenerate whilst the axon itself is preserved. Manifestations, called plaques, may appear in various locations such as the central white matter of the cerebral cortex, optic tracts or spinal cord (Adams 1983). The nature of the degeneration depends on location relative to plaque centres. In the latter are found enlarged extracellular spaces with axons denuded of myelin and reduced numbers of oligodendroglia (Andrews 1972). More distant from the plaque centres some axons are found which have undergone complete demyelination whereas in others there is partial demyelination in which degeneration is restricted to one or several internodes whilst adjacent internodes remain intact. Furthermore, there may be an increased frequency of nodes of Ranvier with a concomitant increase in the number of shorter internodes.

The study of propagation of action potentials in such a variety of geometries is complicated using full nonlinear models, especially when space variables should be treated as continuous. In this note we will focus attention on a simple model which it is hoped can be used to provide some indications as to the effects of patterns of demyelination on transmission in nerve. We will employ the appropriate cable theory which offers the advantage of yielding exact solutions for any number of segments and for any combination of parameters required. However, cable theory has the deficiency of not naturally embracing action potential instigation or propagation so that the methods employed here are mainly useful in the study of localized phenomena. Nevertheless, an approximate but useful study of certain aspects of action potential propagation is possible using threshold criteria, as will be illustrated in the last part of this article.

Model description and notation

Although transmembrane potential differences for neurons can be obtained, in principle, by solving nonlinear systems of differential equations by numerical methods (see for example Tuckwell 1988b), the results for different geometries are difficult to generate and also to present. The paucity of exact theoretical results for the electrophysiological responses of nerve cells renders it desirable to pursue such results when they can be relatively easily obtained. We will illustrate this principle by determining, with the aid of distributed cable theory for nerve segments (as opposed to compartmental models), exact values of the voltage distributions along myelinated axons in the steady state. It is assumed that the axon emanates from a some-dendritic system at one of its ends, whereas at its other extremity is a branching telodendritic system whose nerve terminal endings are presynaptic to a muscle or another nerve cell. As will be demonstrated, the potential distribution along the cable can be found for an arbitrary set of electrophysiological parameters.

The model neuron we are employing has the following components: (i), a cylinder representing a dendritic tree which is assumed to be sealed at the end representing the dendritic terminals; (ii), an R-C circuit representing the soma, this being adjoined to the dendritic cable; (iii), a myelinated axon emanating from the soma and having an initial (unmyelinated) segment, $n-1$ nodes and n internodes; and (iv) a cylinder affixed to the n-th "internode", representing the branching telodendria. With regard to (iv), we are considering a situation which is amenable to the usual mapping procedures from tree to cylinder (Rall 1962; Walsh and Tuckwell 1985) because including the geometric details of a complex telodendritic structure would make the analysis unnecessarily complicated and would yield little, if any, additional insight. The consideration of the telodendritic cable is a feature of the model which has not been previously included.

The various nodes and internodes are not assumed to have the same properties. Although the notation is thereby made a little more cumbersome, one may then address the effects of local changes of the myelin sheath. Since we will consider the important case of a voltage clamp at the soma, it will be unnecessary to describe the responses in the dendritic tree as these will be independent of the responses in the axon and telodendria. All space coordinates are given below in the electrotonic lengths relative to the structure concerned. To apply the results of a calculation it is only necessary to obtain the electrotonic lengths from physical lengths by dividing by the appropriate space (length) constant. The latter can be obtained from resistive and geometric properties. We put:

L_I = electrotonic length of the initial segment;
L_T = electrotonic length of the telodendritic cable;
L_k = electrotonic length of the k-th internode, $k=1, 2, \ldots, n$;
S_k = electrotonic length of the k-th node, $k=1, 2, \ldots, n-1$;
$U(X)$ = electrical potential at points whose distance is X along the initial segment, $0 \leq X \leq L_I$;
$V(Y)$ = electrical potential at points whose distance is Y along the telodendritic cable, $0 \leq Y \leq L_T$;
$U_k(X_k)$ = electrical potential at points whose distance is X_k along the k-th internode, $0 \leq X_k \leq L_k$, $k=1, 2, \ldots, n$;
$V_k(Y_k)$ = electrical potential at points whose distance is Y_k along the k-th node, $0 \leq Y_k \leq M_k$, $k=1, 2, \ldots, n-1$.

Furthermore, we let the reciprocals of the internal resistances of characteristic lengths of the various cable segments be as follows:

g, for the initial segment;
g_k, for the k-th internode, $k=1, 2, \ldots, n$;
γ, for the cable representing the telodendria;
γ_k, for the k-th node, $k=1, 2, \ldots, n-1$.

The reciprocals of these quantities (conductances) are introduced because they occur frequently in the calculations.

Determination of the voltage distribution

Under the above assumptions, the voltage over the various segments satisfies a second order differential equa-

tions whose solutions are well-known (see for example Tuckwell 1988 a). Then we have on the initial segment and telodendritic cable,

$U(X)=a\cosh X+b\sinh X$,
$V(Y)=c\cosh Y+d\sinh Y$,

whereas on the internodes and nodes,

$U_k(X_k)=a_k\cosh X_k+b_k\sinh X_k$,
$V_k(Y_k)=c_k\cosh Y_k+b_k\sinh Y_k$,

where a, b, c, d and the a_k, b_k, c_k, d_k are constants to be determined by applying the following boundary conditions.

A *Voltage clamp at the soma*

Putting $X=0$ and assuming the soma is clamped at V_s, we must have

$a=V_s$.

B *Continuity of potential*

At the junction of the initial segment with the first internode, continuity of potential implies $U(L_I)=U_1(0)$ so that

$a\cosh L_I+b\sinh L_I=a_1$.

Applying the same condition at the junction of the k-th internode with the k-th node yields

$a_k\cosh L_k+b\cosh L_k=c_k$,

where k varies from 1 to $n-1$. Further application at the junction of the k-th node with the $(k+1)$-th internode, gives

$c_k\cosh M_k+d_k\sinh M_k=a_{k+1}$,

for values of k from 1 n-1. Finally, for continuity of potential at the junction of the n-th internode and the telodendritic cable, we require

$a_n\cosh L_n+b_n\sinh L_n=c$.

C *Conservation of current*

At the junction of the initial segment with the first internode, conservation of axial current requires that $gU'(L_I)=g_1U_1'(0)$. Upon substituting the above expressions for U and U_1 this gives

$g(a\sinh L_I+b\cosh L_I)=g_1b_1$.

Similarly by considering the junction of the k-th internode with the k-th node,

$g_k(a_k\sinh L_k+b_k\cosh L_k)=\gamma_k d_k$,

where k varies from 1 to $n-1$. Current conservation at the k-th node, $(k+1)$-th internode junction yields

$\gamma_k(c_k\sinh M_k+d_k\cosh M_k)=g_{k+1}b_{k+1}$,

with k between 1 and $n-1$; and at the junction of the n-th internode with the telodendritic cable,

$g_n(a_n\sinh L_n+b_n\cosh L_n)=\gamma d$.

Finally, on employing a sealed-end (zero flux) boundary condition at the remote end of the telodendritic cable, so that $V'(L_T)=0$, the following equation ensues:

$c\sinh L_T+d\cosh L_T=0$.

Altogether there are $4n+2$ constants: a, b, c, d, $a_1,\ldots,a_n, b_1,\ldots,b_n, c_1,\ldots,c_{n-1}, d_1,\ldots,d_{n-1}$, and we have $4n+2$ equations relating these constants. To solve the equations it is convenient to introduce matrix notation. Define the vector $\boldsymbol{x}$ of required constants to have the transpose

$\boldsymbol{x}^T=[a,b,a_1,b_1,c_1,d_1,\ldots,a_{n-1},b_{n-1},c_{n-1},d_{n-1},a_n,b_n,c,d]$

and the vector $\boldsymbol{b}$ with transpose

$\boldsymbol{b}^T=[V_s,0,0,\ldots,0]$,

which also has $4n+2$ components. Then the above $4n+2$ equations can be described by the matrix equation

$\mathbf{A}\,\boldsymbol{x}=\boldsymbol{b}$.

Before defining the matrix $\mathbf{A}$, we introduce for brevity,

$C_I=\cosh L_I$, $S_I=\sinh L_I$, $C_k=\cosh L_k$, $S_k=\sinh L_k$,

and

$D_k=\cosh M_k$, $T_k=\sinh M_k$, $C_T=\cosh L_T$, $S_T=\sinh L_T$.

Then $\mathbf{A}$ is the following $(4n+2)\times(4n+2)$ matrix:

$$\begin{pmatrix}
1 & 0 & 0 & 0 & 0 & 0 & \cdot & \cdot & \cdot & \cdot & \cdot & \cdot & \cdot & 0 & 0\\
C_I & S_I & -1 & 0 & 0 & 0 & \cdot & \cdot & \cdot & \cdot & \cdot & \cdot & \cdot & 0 & 0\\
gS_I & gC_I & 0 & -g_1 & 0 & 0 & \cdot & \cdot & \cdot & \cdot & \cdot & \cdot & \cdot & 0 & 0\\
\cdot & \cdot & \cdot & \cdot & \cdot & \cdot & \cdot & \cdot & \cdot & \cdot & \cdot & \cdot & \cdot & \cdot & \cdot\\
\cdot & \cdot & \cdot & \cdot & \cdot & C_k & S_k & -1 & 0 & 0 & 0 & \cdot & \cdot & \cdot & \cdot\\
\cdot & \cdot & \cdot & \cdot & \cdot & g_kS_k & g_kC_k & 0 & -\gamma_k & 0 & 0 & \cdot & \cdot & \cdot & \cdot\\
\cdot & \cdot & \cdot & \cdot & \cdot & 0 & 0 & D_k & T_k & -1 & 0 & \cdot & \cdot & \cdot & \cdot\\
\cdot & \cdot & \cdot & \cdot & \cdot & 0 & 0 & T_k\gamma_k & D_k\gamma_k & 0 & -g_{k+1} & \cdot & \cdot & \cdot & \cdot\\
\cdot & \cdot & \cdot & \cdot & \cdot & \cdot & \cdot & \cdot & \cdot & \cdot & \cdot & \cdot & \cdot & \cdot & \cdot\\
\cdot & \cdot & \cdot & \cdot & \cdot & \cdot & \cdot & \cdot & \cdot & \cdot & \cdot & \cdot & \cdot & \cdot & \cdot\\
0 & 0 & \cdot & \cdot & \cdot & \cdot & \cdot & \cdot & \cdot & \cdot & 0 & C_n & S_n & -1 & 0\\
0 & 0 & \cdot & \cdot & \cdot & \cdot & \cdot & \cdot & \cdot & \cdot & 0 & g_nS_n & g_nC_n & 0 & -\gamma\\
0 & 0 & \cdot & \cdot & \cdot & \cdot & \cdot & \cdot & \cdot & \cdot & 0 & 0 & 0 & S_T & C_T
\end{pmatrix}$$

Here the first and last three rows of **A** are given explicitly. The inner sub-matrix displayed has as its upper-left corner element, the element in the $4k$-th row and $(4k-1)$-th column of **A**. All other elements are zeros.

Solving a linear system is efficiently performed if the coefficient matrix is trigidiagonal in form. Before transforming **A** to this form we introduce some further constants:

$$A_I = g/C_I,\ B_I = g S_I/C_I,\ A_k = g_k/C_k,$$
$$B_k = g_k S_k/C_k,\ E_k = \gamma_k/D_k,\ F_k = \gamma_k T_k/D_k,$$

where k varies from 1 to $n-1$. Then the above system takes the form $\mathbf{B}\boldsymbol{x} = \boldsymbol{b}$, with $\boldsymbol{b}$ being unaffected by the transformation and where **B** is the tridiagonal matrix,

$$\begin{pmatrix}
1 & 0 & 0 & 0 & 0 & \cdot & \cdot & \cdot & \cdot & \cdot & \cdot & \cdot & \cdot & 0 & 0 \\
C_I & S_I & -1 & 0 & 0 & \cdot & \cdot & \cdot & \cdot & \cdot & \cdot & \cdot & \cdot & 0 & 0 \\
0 & A_I & B_I & -g_1 & 0 & \cdot & \cdot & \cdot & \cdot & \cdot & \cdot & \cdot & \cdot & 0 & 0 \\
\cdot & \cdot & \cdot & \cdot & \cdot & \cdot & \cdot & \cdot & \cdot & \cdot & \cdot & \cdot & \cdot & \cdot & \cdot \\
\cdot & \cdot & \cdot & \cdot & \cdot & \cdot & \cdot & \cdot & \cdot & \cdot & \cdot & \cdot & \cdot & \cdot & \cdot \\
\cdot & \cdot & \cdot & \cdot & C_k & S_k & -1 & 0 & 0 & 0 & \cdot & \cdot & \cdot & \cdot & \cdot \\
\cdot & \cdot & \cdot & \cdot & 0 & A_k & B_k & -\gamma_k & 0 & 0 & \cdot & \cdot & \cdot & \cdot & \cdot \\
\cdot & \cdot & \cdot & \cdot & 0 & 0 & D_k & T_k & -1 & 0 & \cdot & \cdot & \cdot & \cdot & \cdot \\
\cdot & \cdot & \cdot & \cdot & 0 & 0 & 0 & E_k & F_k & -g_{k+1} & \cdot & \cdot & \cdot & \cdot & \cdot \\
\cdot & \cdot & \cdot & \cdot & \cdot & \cdot & \cdot & \cdot & \cdot & \cdot & \cdot & \cdot & \cdot & \cdot & \cdot \\
0 & 0 & \cdot & \cdot & \cdot & \cdot & \cdot & \cdot & \cdot & \cdot & \cdot & C_n & S_n & -1 & 0 \\
0 & 0 & \cdot & \cdot & \cdot & \cdot & \cdot & \cdot & \cdot & \cdot & \cdot & 0 & A_n & B_n & -\gamma \\
0 & 0 & \cdot & \cdot & \cdot & \cdot & \cdot & \cdot & \cdot & \cdot & \cdot & 0 & 0 & S_T & C_T
\end{pmatrix},$$

The required solution vector $\boldsymbol{x}$ can now be easily obtained recursively (Thomas' method, see for example Tuckwell 1988 b).

Applications

An exact calculation for $n=1$

Suppose there is just one internode adjoining a soma-dendritic system at one end and a branching synaptic terminal structure at the other. Thus $n=1$ and there are six equations for the six constant a, b, a_1, b_1, c and d. On the initial segment the depolarization is

$$U(X) = a \cosh X + b \sinh X,\ X \in [0, L_I],$$

whereas on the internode it is

$$U_1(X_1) = a_1 \cosh X_1 + b_1 \sinh X_1,\ X_1 \in [0, L_1],$$

and on the telodendritic cable it is

$$V(Y) = c \cosh Y + d \sinh Y,\ Y \in [0, L_T].$$

The tridiagonal matrix **B** has 6 rows and columns and the corresponding system can be solved explicitly. The coefficients required are as follows:

$$d = \frac{-A_1 \Gamma S_T}{C_T (B_1 \beta + A_1 \alpha) + S_T \gamma \beta}$$

$$c = \frac{A_1 \Gamma + \gamma \beta d}{B_1 \beta + A_1 \alpha}$$

$$b_1 = \frac{\alpha c - \Gamma}{\beta}$$

$$a_1 = \frac{A_I C_I V_s + g_1 S_I b_1}{\alpha}$$

$$b = \frac{a_1 - C_1 V_s}{S_I}$$

$$a = V_s,$$

where we have defined

$$\alpha = B_I S_I + A_I$$
$$\beta = S_1 D + C_1 g_1 S_I$$
$$\Gamma = C_1 A_I C_I V_s.$$

To evaluate these expressions it is desirable to have physiological values of the parameters, g, g_1, γ, and the electronic lengths L_I, L_1, L_T. There is a paucity of such data, but a cell with properties similar to a typical mammalian peripheral nervous system fibre with overall diameter 13 μ was chosen for consideration. Based on the information available (Rall 1977; Ritchie 1984 a, b) it was assumed that characteristic lengths were 300 μ for the initial segment and telodendritic cable and 1.2 cm for the myelinated internode. Hence the following values were adopted; $L_I = 0.3$, $L_1 = 0.1$ and $L_T = 0.6$, corresponding to physical lengths of 1.2 mm for the myelinated internode, 90 μ for the initial segment and 180 μ for the telodendritic cable. The remaining parameters were set at $g = 10^{-6}$, $g_1 = 10^{-7}$ and $\gamma = 10^{-6}$. The upper (solid) curve in Figure 1 A shows the potential distribution along the neuron from soma to synaptic terminals when a voltage clamp of $V_s = 10$ mV is applied at the soma. (Note that the results are proportional to V_s because of the linearity of the model.) The length scale in this figure is in physical units (μ) and is not electrotonic. The potential drop across the internode is only about 3 mV which is the same order of magnitude as the

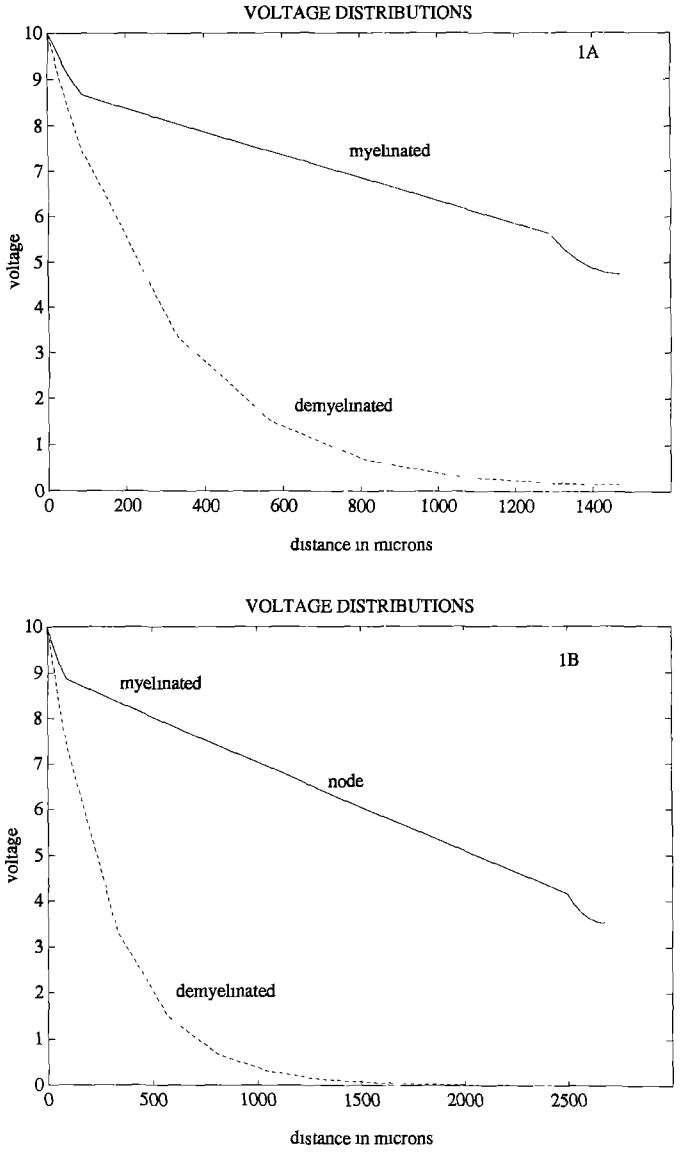

Fig. 1. **A** Calculated voltage distribution from the soma to the synaptic terminals in the case of one internode with and without myelin. Here and in figures 1 B and 2, voltages are in millivolts with the somatic voltage fixed at 10 mV. **B** Voltage distribution in the case of two myelinated internodes and when the myelin is removed. The word "node" marks the position of the node

drop on both the initial segment and telodendria, even though the internode is about ten times as long. The effects of removing the myelin sheath entirely are dramatic and are shown in the dashed curve of Fig. 1 A. Here, for the same physical dimensions and all other parameters the same except for the characteristic length of the internode, so that L_1 is now 4.0, the voltage is greatly reduced, by up to a factor of thirty at the end of the telodendritic cable.

Computer-generated solutions for $n \geq 2$

Figure 1 B shows the voltage along the axon in the case of two internodes. The upper curve is for the case of intact myelin sheaths, where now there is a node of Ranvier (at

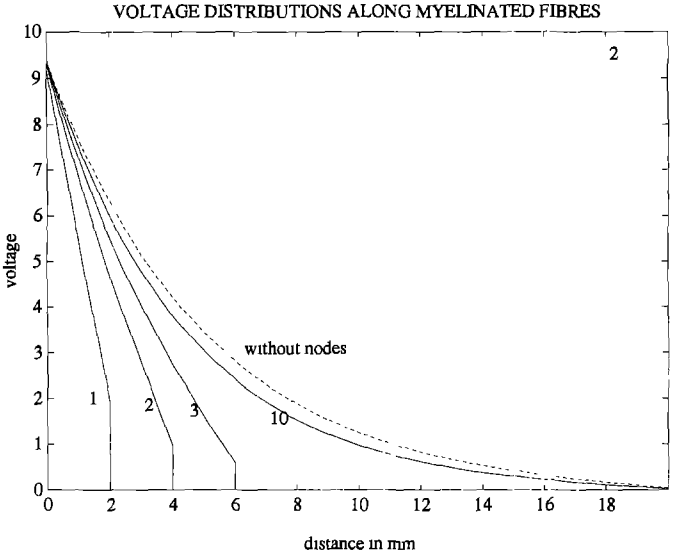

Fig. 2. Voltage distributions along the axon in the cases of 1, 2, 3 and 10 myelinated internodes. The dashed line is the calculated potential when the nodes are ignored

the position marked "node") whose physical length was taken as 3 μ and whose electrotonic length is $S_1 = 0.01$. The value of γ_1 was set at 10^{-6}. Notice that the voltage at the synaptic terminals is not significantly changed, even though the length of the axon has been approximately doubled. The lower curve in Figure 1 B shows the dramatic effects of demyelination. In this case the voltage at the synaptic terminals is enhanced by a factor of over 1000 by the presence of myelin.

Figure 2 illustrates the effect of adding more internodes, all of which are assumed to be myelinated. Here each internode is assumed to be 2000 μ and to have a characteristic length of 0.5 cm and $g_k = (7 \times 10^7)^{-1}$ for all k. Because the telodendritic cable is so short compared with the fibre length, it is not possible to discern the zero derivative boundary condition at the terminal. It can be seen that the drop in potential is approximately exponential along the entire structure when the number of internodes becomes 10. The upper curve in this figure is the result of the calculation for 10 internodes when the nodes themselves have been taken out: that is, a uniform myelinated cable. It can be seen that the voltage distribution is very little affected.

We also investigated the effect of varying the position of one demyelinated segment. To do this it was assumed that an action potential had in fact propagated to the k-th node from the synaptic terminals (i.e., node $n-k$), thus making $V_k(M_k) = 100$ mV (this voltage affecting the calculations proportionally) and that the internode immediately closer to the terminals (i.e., internode $n-k+1$) was completely demyelinated. The question was whether demyelination would be more deleterious closer to the telodendria. Figure 3 shows how the depolarization, $U_{n-k+1}(L_{n-k+1})$, at the end of the missing internode changes as k increases. (The smaller k is, the closer the missing myelin to the synaptic terminals). It can be seen that although the voltage at the end of the missing myelin is more adversely affected when k is small, the difference

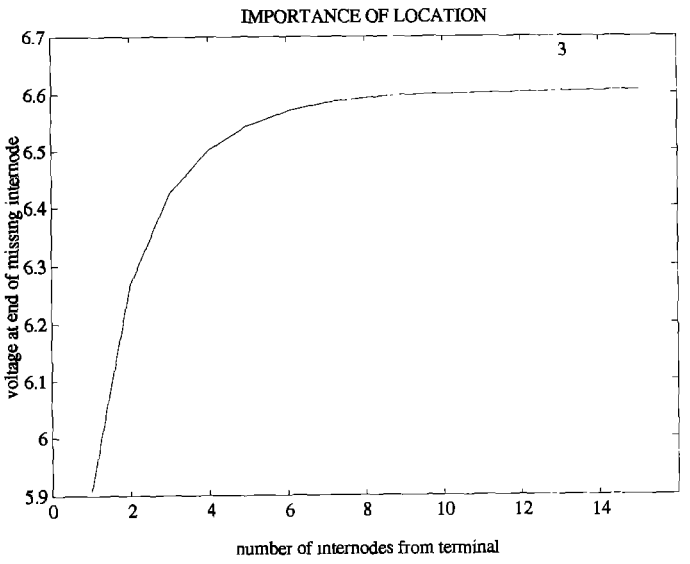

Fig. 3. Showing the effects of the position of one demyelinated segment on the voltage at the terminals. For details of the calculation, see text

is only about 10% as the position of the demyelinated segment changes from being extremely close to the terminals to being proximal to the cell body. Assuming a threshold of about 10 mV for action potential generation at the next active site, the cable calculations indicate propagation failure regardless of the location of the missing myelin, although a missing segment of myelin closer to the terminals has a somewhat more negative effect than a missing segment further upstream.

An approximate upper bound for internodal length

When a nerve impulse propagates from a zone near the cell body to the synaptic terminals, the action potential is renewed at each node. Thus the signal at, say, the k-th node from the cell body must generate at least a threshold signal at the $(k+1)$-th node. Working approximately with voltage criteria, let us assume a peak voltage of V_p and a threshold voltage of V_θ. Now from points remote from the synaptic terminals the axon further on acts like a semi-infinite one. If the voltage at a node is V_p, then the signal at distance x cm further along is roughly

$$V(x) = V_p \, e^{-x/\lambda},$$

where λ is the length constant. Note that we are considering the potential at the beginning and end of an internode so that only the length constant for the internode is involved. Letting the internodal length be L, we require for a threshold crossing at the next node,

$$V_p \, e^{-L/\lambda} > V_\theta .$$

Rearranging this inequality leads to the approximate requirement

$$L < \lambda \ln\left(\frac{V_p}{V_\theta}\right),$$

which provides an upper bound for the internodal length. Since λ is expressible in terms of fundamental physical constants (resistivities, membrane thickness and axonal diameter), this gives an approximate upper limit for the internodal length in a myelinated nerve in terms of those constants. For example, Rubinstein (1991) employed a length constant of $\lambda = 589$ μ, which, on using the standard values $V_p = 100$ mV and $V_\theta = 10$ mV, gives the approximate upper bound of 1.36 mm for the internodal length. This is very close to reported figures for the internodal distance.

References

Adams CWM (1983) The general pathology of multiple sclerosis: morphological and chemical aspects of lesions. In: Hallpike JF, Adams CWM, Tourtellotte WW (eds). *Multiple Sclerosis,* Chapman and Hall, London, pp 203–240

Andrews JM (1972) The ultrastructural neuropathology of multiple sclerosis. In: Wolfgram F, Ellison GW, Stevens JG, Andrews JM (eds). *Multiple Sclerosis,* Academic Press, New York, pp 23–52

Bell J (1980) Some threshold results for models of myelinated nerves. Math Biosci 54:181–190

BeMent SL, Ranck JR, Jr (1969) A quantitative study of electrical stimulation of central myelinated fibers. Exptl Neurol 24:147–170

BeMent SL, Ranck JR, Jr (1969) A model for electrical stimulation of central myelinated fibers with monopolar electrodes. Exptl Neurol 24:171–186

Chen P-L (1992) Qualitative analysis of myelinated nerve fibers with point-node Fitzhugh-Nagumo dynamic system. SIAM J Math Anal 23:81–98

Dodge FA, Frankenhaeuser B (1958) Membrane currents in isolated frog nerve fibre under voltage clamp conditions. J Physiol 143:76–90

Frankenhaeuser B, Huxley AF (1964) The action potential of the myelinated nerve fibre under voltage clamp conditions. J Physiol 143:76–90

Frankenhaeuser B, Huxley AF (1964) The action potential of the myelinated nerve fibre of *Xenopus laevis* as computed on the basis of voltage clamp data. J Physiol 171:302–315

Hodgkin AL, Huxley AF (1952) A quantitative description of membrane current and its application to conduction and excitation in nerve. J Physiol 117:500–544

Koide FT (1975) Electrotonus in medullated nerve. Math Biosci 25:363–373

Koles ZJ, Rasminsky M (1972) A computer simulation of conduction in demyelinated nerve fibres. J Physiol 227:351–364

Moore JW, Joyner RW, Brill MH, Najar-Joa M (1978) Simulations of conduction in uniform myelinated fibers. Biophys J 21:147–160

Rall W (1962) Theory of physiological properties of dendrites. Ann NY Acad Sci 96:1071–1092

Rall W (1977) Core conductor theory and cable properties of nedurons. In: Kandell ER (Ed), *Handbook of Physiology. The Nervous System,* Vol 1, American Physiological Society, Bethesda

Rasminsky M, Sears TA (1972) Internodal conduction in undissected demyelinated nerve fibres. J Physiol 227:323–350

Ritchie JM (1984a) Physiological basis of conduction in myelinated nerve fibers. In: Morell P (ed), *Myelin.* Plenum Press, New York pp 117–145

Ritchie JM (1984b) Pathophysiology of conduction in demyelinated nerve fibers. In: Morell P (ed), *Myelin.* Plenum Press, New York, pp 337–367

Rubinstein JT (1991) Analytical theory for extracellular electrical stimulation of nerve with focal electrodes. Biophys J 60:538–555

Rushton WAH (1951) A theory of the effects of fibre size in medullated nerve. J Physiol 115:101–122

Scott AC (1964) Analysis of a myelinated nerve model. Bull Math Biophys 26:247–254

Tuckwell HC (1988a) *Introduction to Theoretical Neurobiology,* Vol 1, *Linear Cable Theory and Dendritic Structure,* Cambridge University Press, New York

Tuckwell HC (1988b) *Introduction to Theoretical Neurobiology,* Vol 2, *Nonlinear and Stochastic Theories.* Cambridge University Press, New York

Walsh JB, Tuckwell HC (1985) Determination of the electrical potential over dendritic trees by mapping onto a nerve cylinder. J Theoret Neurobiol 4:27–46

Waxman SG, Brill MH (1978) Conduction through demyelinated plaques in multiple sclerosis: computer simulations of facilitation by short internodes. J Neurol Neurosurg Psychiatry 41:408–416